Optimization of Mechanical Properties of PP/Nanoclay/$CaCO_3$ Ternary Nanocomposite Using Response Surface Methodology

Yasser Zare, Hamid Garmabi, Farhad Sharif

Department of Polymer Engineering and Color Technology, Amirkabir University of Technology, Tehran, Iran

Received 18 August 2010; accepted 13 February 2011
DOI 10.1002/app.34378
Published online 8 July 2011 in Wiley Online Library (wileyonlinelibrary.com).

ABSTRACT: Response surface method of experimental design was applied to optimize the mechanical properties of polypropylene (PP)/nanoclay/$CaCO_3$ hybrid ternary nanocomposite using three different levels of melt flow index (MFI) of PP, nanoclay, and $CaCO_3$ contents. The samples were prepared by melt mixing in a lab scale corotating twin screw extruder. The main effect of each parameter on the tensile modulus, tensile strength, and impact strength was extensively discussed. The structure of obtained nanocomposite was studied using X-ray diffraction (XRD), atomic force microscopy (AFM), and scanning electron microscopy (SEM) techniques. Tensile modulus and impact resistance of prepared ternary nanocomposite were correlated to considered parameters using a second-order polynomial model. Also, the optimum values of studied variables were determined using contour plots. The obtained results show that increasing the nanoclay and $CaCO_3$ contents improve the tensile modulus up to 45%, whereas the optimum value of impact strength, about 54%, is achieved at low concentrations of nanoclay (2 wt %) and $CaCO_3$ (8 wt %). © 2011 Wiley Periodicals, Inc. J Appl Polym Sci 122: 3188–3200, 2011

Key words: ternary nanocomposite; mechanical properties; response surface methodology

INTRODUCTION

Polypropylene (PP) is one of the mainly used polymers in different areas such as automobile, household goods, packaging, and textile industries because of their attractive properties such as good performance, ease of processability, and low cost. However, several weaknesses of PP including low stiffness, low toughness, and low service temperature limit its application. Therefore, there is much focusing on the PP-based nanocomposites to improve their mechanical and thermal properties.

Nanoclay is a commonly used nanofiller in polymer nanocomposites causing a major improvement in the mechanical, thermal, and barrier properties relatively at low content.[1–4] To increase interaction between nanoclay and PP, compatibilizer or surface modification of nanoparticles is applied. The maleic anhydride grafted polypropylene (PPgMA) has been used as a compatibilizer to enhance the adhesion between nanoclay and PP matrix and promote the intercalated/exfoliated structure.[5,6]

Calcium carbonate ($CaCO_3$) is also usual filler developing the mechanical properties of polymers, especially the toughness due to the distinct growth in the interfacial area between the filler and the matrix.[7–9] When $CaCO_3$ nanoparticles are added to the polymer matrix, agglomeration of nanoparticles occurs owing to high surface energy. Therefore, treatment of $CaCO_3$ nanoparticles is performed applying stearic acid or titane coupling agent to increase the interface adhesion between nanoparticles and matrix resulting to good dispersion of $CaCO_3$ nanoparticles in polymer matrix.[10,11]

Recently, it has been shown that the presence of two nanofillers affects the overall properties of ternary nanocomposite.[12–14] This approach creates very exceptional features in behavior study of nanocomposite. Chen et al.[12] have found that coexistence of nanoclay and nano-$CaCO_3$ at low loading improved the tensile modulus of PP but reduced the impact strength. Tang et al.[13] also studied the PP/montmorillonite/$CaCO_3$ ternary nanocomposite and concluded that the ternary nanocomposite has better mechanical and thermal properties in comparison with binary nanocomposites.

In the recent years, response surface methodology has been applied successfully for optimization of various parameters.[15–18] The advantage of this method is reduction of the total number of experiments, whereas mutual influences of many variables are investigated. Generally, response surface method facilitates the obtaining an overview of the influential parameters. This method is briefly explained in the next section.

Correspondence to: H. Garmabi (garmabi@aut.ac.ir).

TABLE I
Levels of Studied Variables

Variables	Level 1	Level 2	Level 3
x_1, MFI of PP (g/10 min)	4	10	16
x_2, Nanoclay content (wt %)	2	4	6
x_3, $CaCO_3$ content (wt %)	8	14	20

Response surface methodology

Response surface methodology is a collection of mathematical and statistical techniques useful for modeling and analysis of problems in which a response of interest is affected by several parameters. The objective is to determine optimal conditions for the factors that have the most influence on the results of interest.

The most extensive applications of this method are in the particular situations where several input variables potentially influence some performance measures of the process. The performance measure is called the response. The input variables are sometimes called independent variables, and they are subject to the control of the experimenter. The field of response surface methodology consists of the experimental strategy for exploring the space of the process or independent variables, empirical statistical modeling to develop an appropriate approximating relationship between the yield and the process variables, and optimization methods for finding the values of the process variables that produce desirable values of the response.[19,20] The second-order model is extensively used in response surface methodology given by:

$$Y = \beta_0 + \sum_{i=1}^{k} \beta_i x_i + \sum_{i=1}^{k} \beta_{ii} x_i^2 + \sum \sum_{i<j-2}^{k} \beta_{ij} x_i x_j + \varepsilon \quad (1)$$

where β_{ii} is the curvature term of independent variables, β_{ij} is the interaction coefficient between variables x_i and x_j, k is the number of factors, and ε shows the random error in Y. The correlation between the response and the variables is visualized by this model to compare the influence of the parameters and to predict the results for other values of variables.

Box Behnken system has been used in the current study to design the experiments. The designs are produced by combination of two-level factorial designs. In the current work, melt flow index (MFI) of PP, nanoclay, and $CaCO_3$ contents was considered as three variables presented in Table I. Response surface method produces 15 experiments that formulation designs are shown in Table II. The samples are represented as PP$n/x/y$, where n is MFI of PP matrix, x is the weight percent of nanoclay, and y is the weight percent of $CaCO_3$.

This method designs excess formulations in the average levels of all parameters to minimize the operational errors, sufficiently.[19] Therefore, PP10/4/14 sample is repeated three times in Table II.

In this article, response surface methodology was used to optimize the material parameters including MFI of PP, nanoclay, and $CaCO_3$ contents to produce PP/nanoclay/$CaCO_3$ ternary nanocomposite presenting high tensile modulus, tensile, and impact strength.

EXPERIMENTAL

Materials

Three grades of mono-dispersed PP homopolymer were used in this study. PP4 (Turkmen plast TNGIZT, MFI = 4 g/10 min, 230°C, 2.16 kg) was supplied from Turkmen bashi refinery, Turkmenistan, PP10 (ZH500, MFI = 10 g/10 min, 230°C, 2.16 kg) was received from Navid Zar Shimi Petrochemical Company, Iran, and PP16 (VCS, MFI = 16 g/10 min, 230°C, 2.16 kg) was provided from Marun Petrochemical Company, Iran. Montmorillonite clay modified with a quaternary ammonium salt (Cloisite20A) was received from Southern Clay Products (Singapore). The received clay (montmorillonite) particles are disk-like stacks of silicate layers, 1 nm thick, and varying in diameter from 100 nm to several microns. The layer spacing (*d*-spacing) also is about 2.51 nm. PPgMA PB3150 (MFI = 20 g/10 min, 230°C, 2.16 kg) with 0.5 wt % of maleic anhydride was supplied by Crompton Corp. (Singapore) and precipitated $CaCO_3$ (SOCAL312) was purchased from Solvay (Shanghai, China). The $CaCO_3$ nanoparticles are coated with an organic layer of stearic acid and have the average particle size of 70 nm.

TABLE II
Formulations of Samples According to Response Surface Methodology

Name	MFI of PP	Nanoclay (wt %)	$CaCO_3$ (wt %)
PP10/2/20	10	2	20
PP10/2/8	10	2	8
PP10/6/20	10	6	20
PP10/6/8	10	6	8
PP16/4/8	16	4	8
PP4/2/14	4	2	14
PP4/4/20	4	4	20
PP10/4/14	10	4	14
PP10/4/14	10	4	14
PP16/2/14	16	2	14
PP16/4/20	16	4	20
PP16/6/14	16	6	14
PP10/4/14	10	4	14
PP4/6/14	4	6	14
PP4/4/8	4	4	8

TABLE III
Mechanical Properties of Neat PP Samples

Name	Tensile modulus (GPa)	Tensile strength (MPa)	Impact strength (kJ/m^2)	Fracture energy (J)
PP4	1.75 ± 0.09	37.2 ± 1.14	3.9 ± 0.25	14.5 ± 0.91
PP10	2.17 ± 0.12	40 ± 1.28	2.5 ± 0.21	7.22 ± 0.82
PP16	1.85 ± 0.08	37.1 ± 1.02	3.15 ± 0.28	8.4 ± 0.73

Preparation of ternary nanocomposite

First, all materials were dried at 80°C for 10 h. According to the designed formulations, the materials were dry-mixed. The content of PPgMA was considered equally to nanoclay concentration in all samples. The melt mixing was carried out using a lab scale corotating twin screw extruder, Brabender TSE 20/40D (D = 20 mm, L/D = 40). The screw speed was kept at 250 rpm, and the feeding rate was maintained at 3 kg/h. The temperature profile was set at 210, 215, 220, 225, and 230°C from hopper to die, respectively. The injection molding of extruded samples was performed using a MonoMat 80 injection molding machine at melt temperature of 245°C and mold temperature of 80°C.

Characterization

The tensile test was performed according to ASTM D638 using a Z050, Zwick at crosshead speed of 50 mm/min. Reported values are average of at least 5 measurements. Notched charpy impact test was conducted at room temperature by means of an impact tester (Rezilimpactor, Ceast) with pendulum energy of 1 J. At least 10 specimens for each sample were tested. X-ray diffraction (XRD) scans were obtained with a Philips powder diffractometer (model XL30) to study the spacing of nanoclay interlayer and its intensity in prepared nanocomposite. Scanning electron microscopy (SEM) was carried out on a Philips XL30S at 16.0 kV to study dispersion of nanoparticles in polymer matrix. Atomic force microscopy (AFM) analysis was performed using a Universal Scanning Probe Microscopy (C26, DME, Denmark). Si cantilevers with a spring constant of 40N/m were used, and both height and phase images were obtained simultaneously.

RESULTS AND DISCUSSION

Mechanical properties

The mechanical properties of three samples of neat PP are shown in Table III. To better comparing of results, the normalized mechanical properties (obtained result for nanocomposite sample/same result for neat PPn) are presented in Table IV.

The values of coefficients for tensile modulus and impact strength are presented in Table V. The improvement of tensile modulus is observed in all samples attributed to reinforcing effect of nanoclay and $CaCO_3$. The maximum enhancement of tensile modulus occurs in PP4/6/14 sample (45%) and furthermore, the minimum improvement is observed in PP16/4/8 sample by 12%. The improvement of tensile strength is minor, and the maximum enhancement is observed in PP4/6/14 sample by 9%. On other hand, the ultimate reduction of tensile strength is obtained for PP10/6/20 sample by 14%.

TABLE IV
Normalized Results of Mechanical Tests (Normalized Result = Obtained Result for Nanocomposite Sample/Same Result for Neat PP*n*)

Name	Tensile modulus	Tensile strength	Impact strength	Fracture energy
PP10/2/20	1.24 ± 0.02	0.92 ± 0.01	1.3 ± 0.04	0.48 ± 0.02
PP10/2/8	1.14 ± 0.01	0.98 ± 0.02	1.54 ± 0.01	0.54 ± 0.03
PP10/6/20	1.14 ± 0.02	0.86 ± 0.03	1.16 ± 0.02	0.28 ± 0.02
PP10/6/8	1.25 ± 0.03	0.96 ± 0.04	1.29 ± 0.03	0.53 ± 0.01
PP16/4/8	1.12 ± 0.01	0.94 ± 0.02	0.95 ± 0.02	0.4 ± 0.01
PP4/2/14	1.2 ± 0.02	0.99 ± 0.01	1.21 ± 0.03	0.55 ± 0.01
PP4/4/20	1.4 ± 0.01	0.97 ± 0.02	0.97 ± 0.02	0.38 ± 0.03
PP10/4/14	1.15 ± 0.02	0.95 ± 0.03	1.24 ± 0.01	0.42 ± 0.02
PP10/4/14	1.17 ± 0.03	0.98 ± 0.02	1.27 ± 0.02	0.45 ± 0.03
PP16/2/14	1.25 ± 0.02	1 ± 0.03	1.06 ± 0.04	0.41 ± 0.02
PP16/4/20	1.34 ± 0.04	0.96 ± 0.04	0.92 ± 0.01	0.29 ± 0.02
PP16/6/14	1.27 ± 0.02	1.02 ± 0.01	0.94 ± 0.02	0.29 ± 0.03
PP10/4/14	1.13 ± 0.04	0.98 ± 0.02	1.22 ± 0.04	0.4 ± 0.02
PP4/6/14	1.45 ± 0.01	1.09 ± 0.01	0.83 ± 0.02	0.37 ± 0.01
PP4/4/8	1.17 ± 0.01	1.02 ± 0.02	1.26 ± 0.04	0.82 ± 0.03

TABLE V
Coefficient Estimates and *P* Values for Tensile Modulus and Impact Strength Models

Term	Tensile modulus		Impact strength	
	Estimate	*P*	Estimate	*P*
Constant (β_0)	1.150	0.000	1.243	0.000
MFI of PP (β_1)	−0.030	0.362	−0.050	0.054
Nanoclay content (β_2)	0.035	0.294	−0.111	0.003
$CaCO_3$ content (β_3)	0.055	0.125	0.086	0.088
MFI of PP × MFI of PP (β_{11})	0.104	0.065	−0.264	0.001
Nanoclay content × nanoclay content (β_{22})	0.039	0.419	0.032	0.324
$CaCO_3$ content × $CaCO_3$ content (β_{33})	0.004	0.935	0.047	0.169
MFI of PP × Nanoclay content (β_{12})	0.058	0.232	0.065	0.069
MFI of PP × $CaCO_3$ content (β_{13})	0.003	0.955	0.065	0.069
Nanoclay content × $CaCO_3$ content (β_{23})	0.053	0.269	0.028	0.037

The enhancement of impact strength is observed in PP10/2/8 sample by 54%, whereas the maximum reduction of 27% is obtained for PP4/6/14 sample. The influence of each variable on the mechanical properties is individually discussed in the next section.

Effect of MFI of PP

The main effect plots of MFI of PP on the tensile modulus, tensile, and impact strength are presented in Figure 1. Main effect plots show the average values of response at the various levels of other factors. These plots indicate the influence of each parameter on the responses.

The high improvement of tensile modulus (about 31%) is found for samples using the lowest MFI of PP (MFI = 4 g/10 min). The tensile modulus decrease as MFI increase, and the highest reduction is observed in the samples produced with PP MFI of 10 g/10 min. However, by increasing the MFI of PP matrix, tensile modulus improves slightly. As shown in Figure 1(a), a significant effect of MFI of PP matrix on tensile modulus is observed. There is a

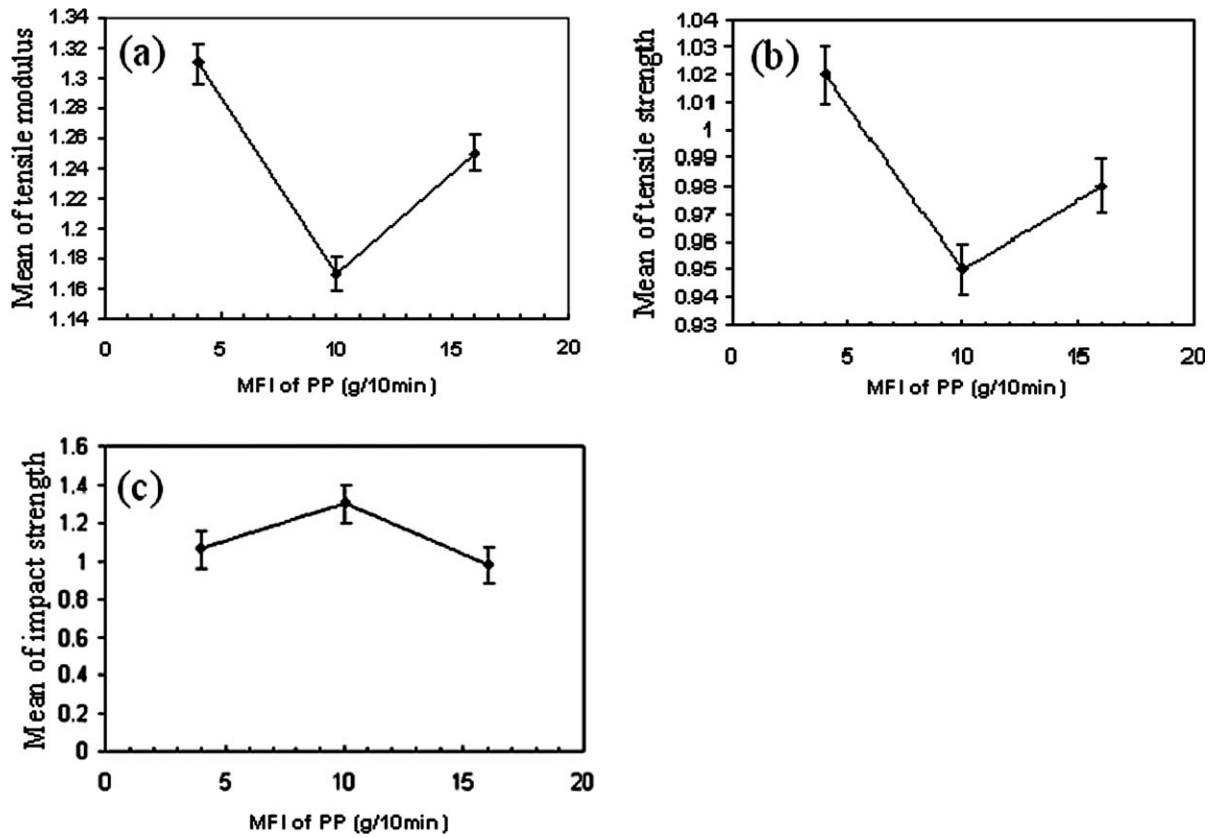

Figure 1 Main effect plots: effect of MFI of PP on (a) tensile modulus, (b) tensile strength, and (c) impact strength.

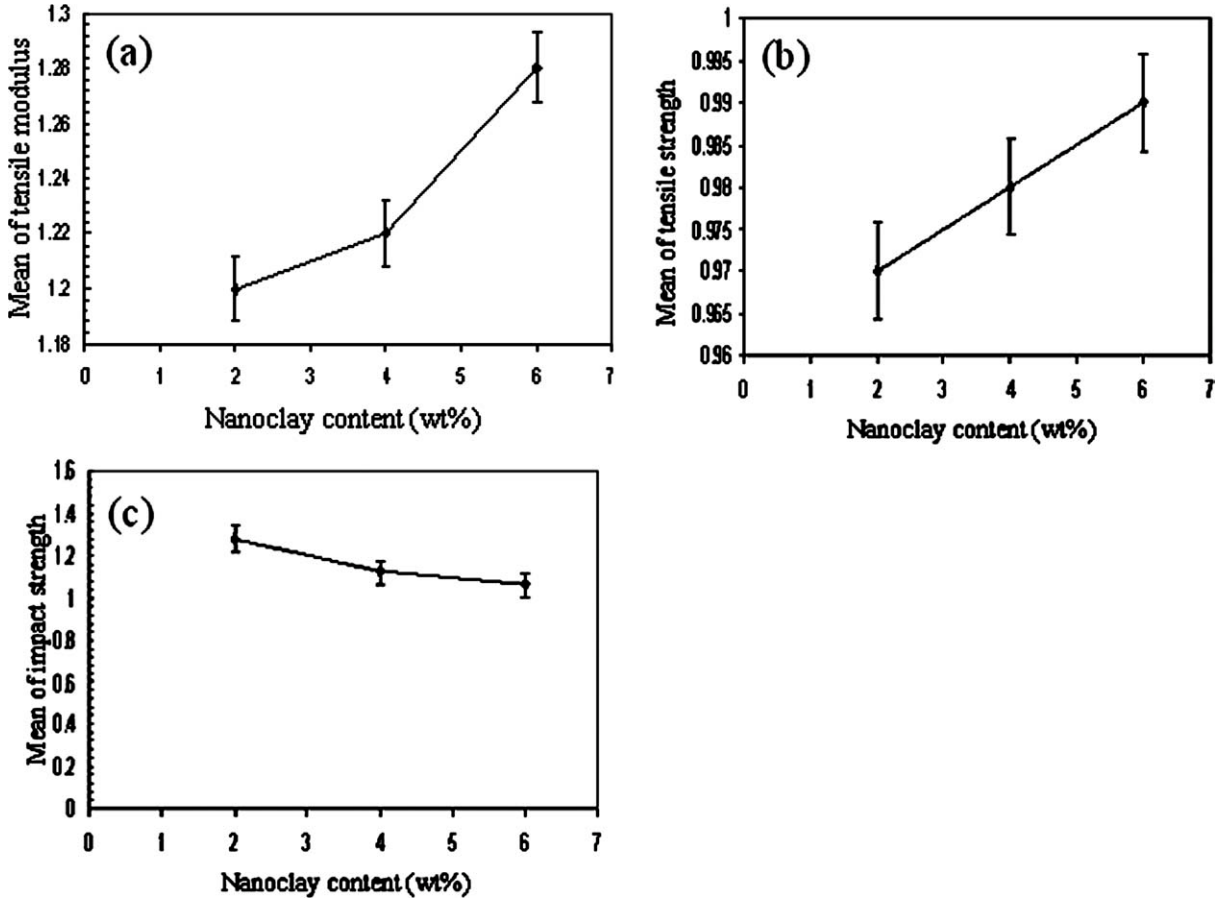

Figure 2 Main effect plots: effect of nanoclay content on (a) tensile modulus, (b) tensile strength, and (c) impact strength.

combination of high shear stress and appropriate molecular diffusion to achieve good dispersion of nanofillers during the melt mixing of nanocomposites as reported in the literature.[12,21–23] High shear stress is needed to break up nanoclay and $CaCO_3$ clusters and to prevent agglomeration due to high surface energy of nanoparticles. This purpose is satisfied using low MFI of polymer matrix or high matrix viscosity. The lack of enough shear stress causes nonuniform dispersion of nanofillers and creates defects in nanocomposite resulting in poor mechanical properties. Using low MFI of PP causes more dispersion of nanoparticles in ternary nanocomposite leading to higher improvement in the tensile modulus. Figure 1(b) shows that the tensile strength variations of prepared nanocomposites with MFI of PP are negligible. The best result of tensile strength is observed for samples using low MFI of PP.

Figure 1(c) indicates that the trend of the impact strength is inversely related to the tensile modulus. The highest impact strength (30%) is obtained for samples including medium MFI of PP. The reduction of impact strength is substantial for samples using higher MFI of PP. The low shear stress attributed to the higher MFI of matrix cause poor dispersion of nanoparticles resulting to large clusters in the system. These clusters act as stress concentration and introduce lower impact resistance in ternary nanocomposite.

Effect of nanoclay content

During the melt processing, nanoclay particles are broken to individual layers with large surface area that interact with polymer matrix molecules effectively producing much ability to load-carrying. The enhancement of modulus even at low content of nanoclay is very considerable.[24–27] The effect of nanoclay content on the tensile properties and impact strength of prepared ternary nanocomposite are presented in Figure 2. It is observed that the tensile modulus increases when nanoclay content increases. The high result of tensile modulus is obtained in the higher level of nanoclay content (6 wt %), whereas the lowest improvement is observed in the nanoclay content of 2 wt %. Furthermore, minor enhancement of tensile strength is evident with increasing of nanoclay concentration.

Also, there is a reverse correlation between nanoclay content and impact strength as shown in Figure 2(c). However, the amount of reduction is negligible due to the toughening effect of nano-$CaCO_3$. The incorporation of nanoclay in polymers often declines

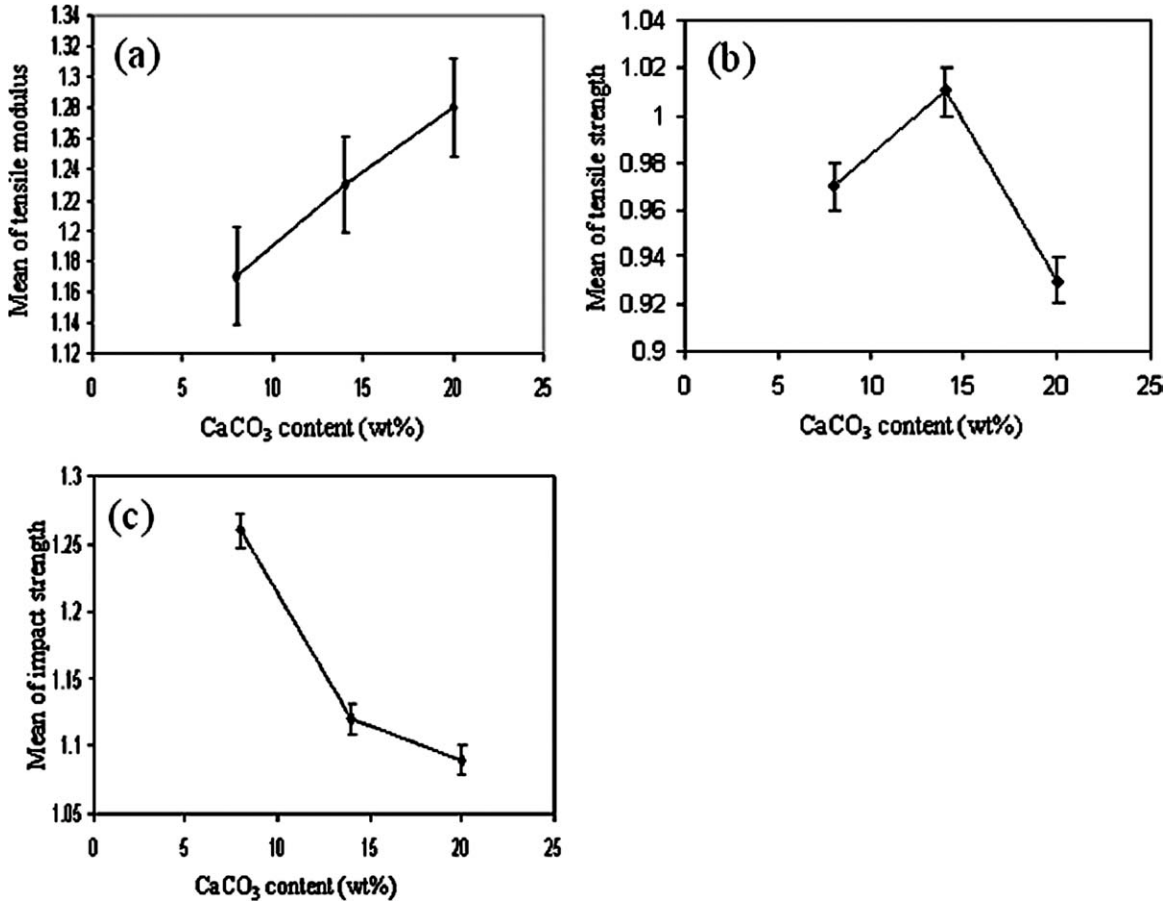

Figure 3 Main effect plots: effect of $CaCO_3$ content on (a) tensile modulus, (b) tensile strength, and (c) impact strength.

the impact strength.[28,29] It is proposed that the lower mobility of PP chains is due to the mechanical involvement of chains with nanoclay layers leading to lower impact resistance at higher nanoclay contents.

Effect of $CaCO_3$ content

$CaCO_3$ nanoparticles enhance the tensile modulus of the polymer matrix, however the intensity of enhancement is lower compared with the nanoclay due to lower surface area of $CaCO_3$ nanoparticles. The enhancement of tensile modulus occurs when efficient adhesion is maintained between the polymer and fillers. The effect of $CaCO_3$ content on the tensile properties and impact strength of hybrid nanocomposite are presented in Figure 3. The $CaCO_3$ content has a noticeably positive influence on the tensile modulus, whereas the tensile strength demonstrates a different trend compared with tensile modulus as shown in Figure 3(b). The tensile strength shows a minor enhancement up to the $CaCO_3$ concentration of 15 wt %. By increasing the level of $CaCO_3$ to 20 wt %, a slight reduction of tensile strength is observed. It is suggested that high content of nanofillers limit the chain movement and also decrease the adhesion at the interface leading to reduced tensile strength. In addition to stiffening effect of $CaCO_3$ nanoparticles, they increase the melt viscosity of the mixture causing more shear stress to the nanoclay layers. The higher shear stress promotes more individual nanoclay layers, i.e., greater level of intercalation and exfoliation as verified previously.[12,30] It is expected that when the amount of $CaCO_3$ increases, the dispersion of nanoclay may enhance greatly. Chen et al.[12] compared the level of intercalation and exfoliation of PP/nanoclay binary and PP/nanoclay/$CaCO_3$ ternary nanocomposite. They have found that the nanoclay exfoliation content in the PP/nanoclay/$CaCO_3$ ternary nanocomposite is obviously much higher than that in PP/nanoclay binary nanocomposite.

The reduction of impact strength with increasing $CaCO_3$ concentration is observed in Figure 3(c). In binary nanocomposites, low content of $CaCO_3$ nanoparticles promote various toughening mechanism leading to higher impact resistance.[8,31] The reduced impact strength in ternary nanocomposite at higher $CaCO_3$ contents could be attributed to the attendance of nanoclay and interaction between two

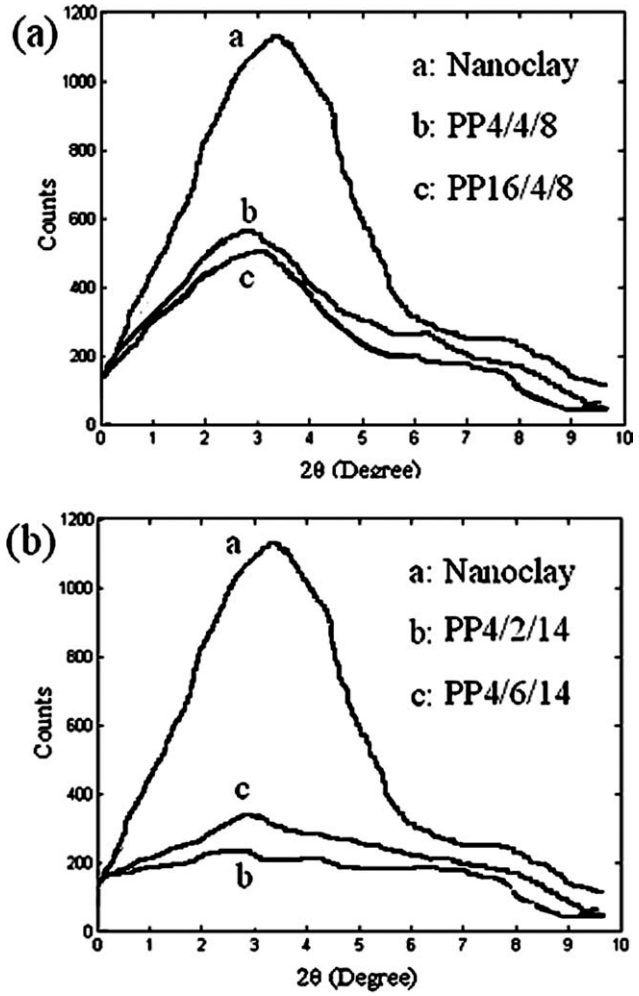

Figure 4 XRD patterns of (a) PP4/4/8 and PP16/4/8 and (b) PP4/2/14 and PP4/6/14 samples.

nanofillers. Furthermore, once the content of $CaCO_3$ increases, the exfoliation level of nanoclay platelets raises that causes restriction of molecular chains mobility. In addition, in the presence of nanoclay layers, good dispersion of high content of $CaCO_3$ layers is not occurred which weaken the nanocomposite.

The main effect plots show the different behavior and the mean improvement level of tensile modulus, tensile, and impact strength in the various levels of parameters. The optimized and the worst levels of parameters can be obtained by these plots for any response. Also, contour plots show the contribution of two factors to obtain the desirable results. The contour plots will be presented later in this article. In addition, response surface methodology cannot suggest the optimized levels of parameters introducing the optimized condition of all responses simultaneously, because the influence of parameters on the responses is different. For example, increasing of nanoclay content in the prepared ternary nanocomposite improve the tensile modulus but decrease the impact strength; therefore, the optimized levels of nanoclay content for tensile modulus and impact strength are 6 and 2 wt %, respectively.

Morphological properties

It is well known that the mechanical properties of nanocomposites are directly related to their structures. The morphology of prepared ternary nanocomposite is studied using XRD, AFM, and SEM analysis. XRD is a suitable method to study the nanocomposite morphology. The nanoclay structure, namely intercalated or exfoliated, may be determined by monitoring the shape, position, and intensity of the basal reflections from the dispersed nanoclay layers.[32]

XRD spectra of pristine nanoclay, PP4/4/8, and PP16/4/8 samples are shown in Figure 4(a). One peak is observed for pristine nanoclay in $2\theta = 3.52^\circ$ relating to interlayer spacing of 2.51 nm. The gallery spacing for PP4/4/8 and PP16/4/8 samples is 2.79

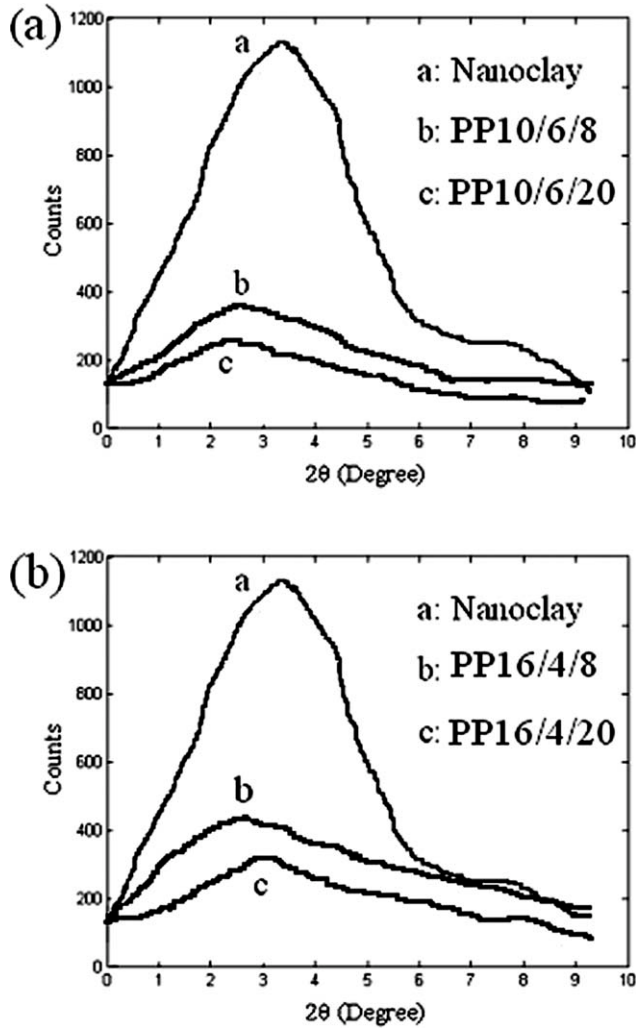

Figure 5 XRD patterns of (a) PP10/6/8 and PP10/6/20 and (b) PP16/4/8 and PP16/4/20 samples.

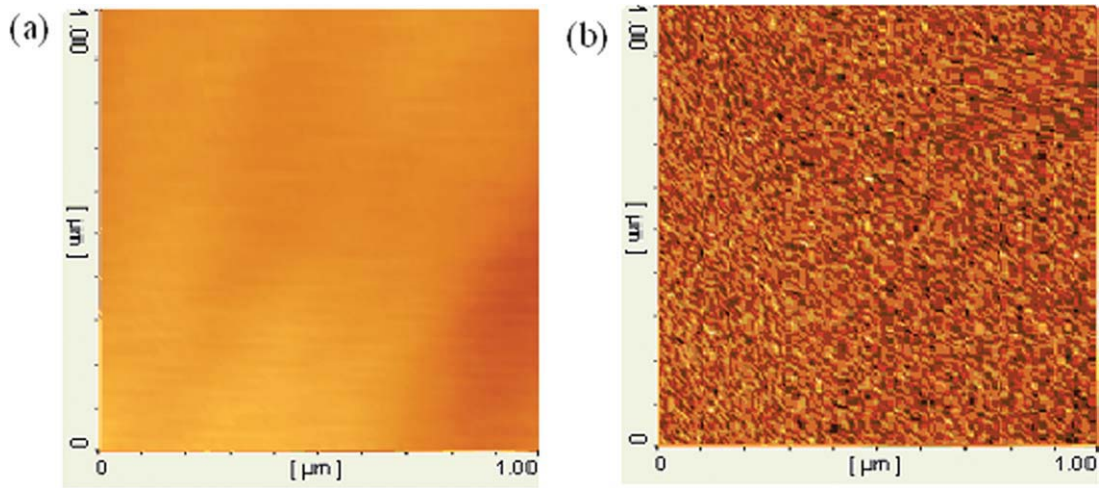

Figure 6 AFM images of PP4 sample: (a) phase and (b) topography images. [Color figure can be viewed in the online issue, which is available at wileyonlinelibrary.com.]

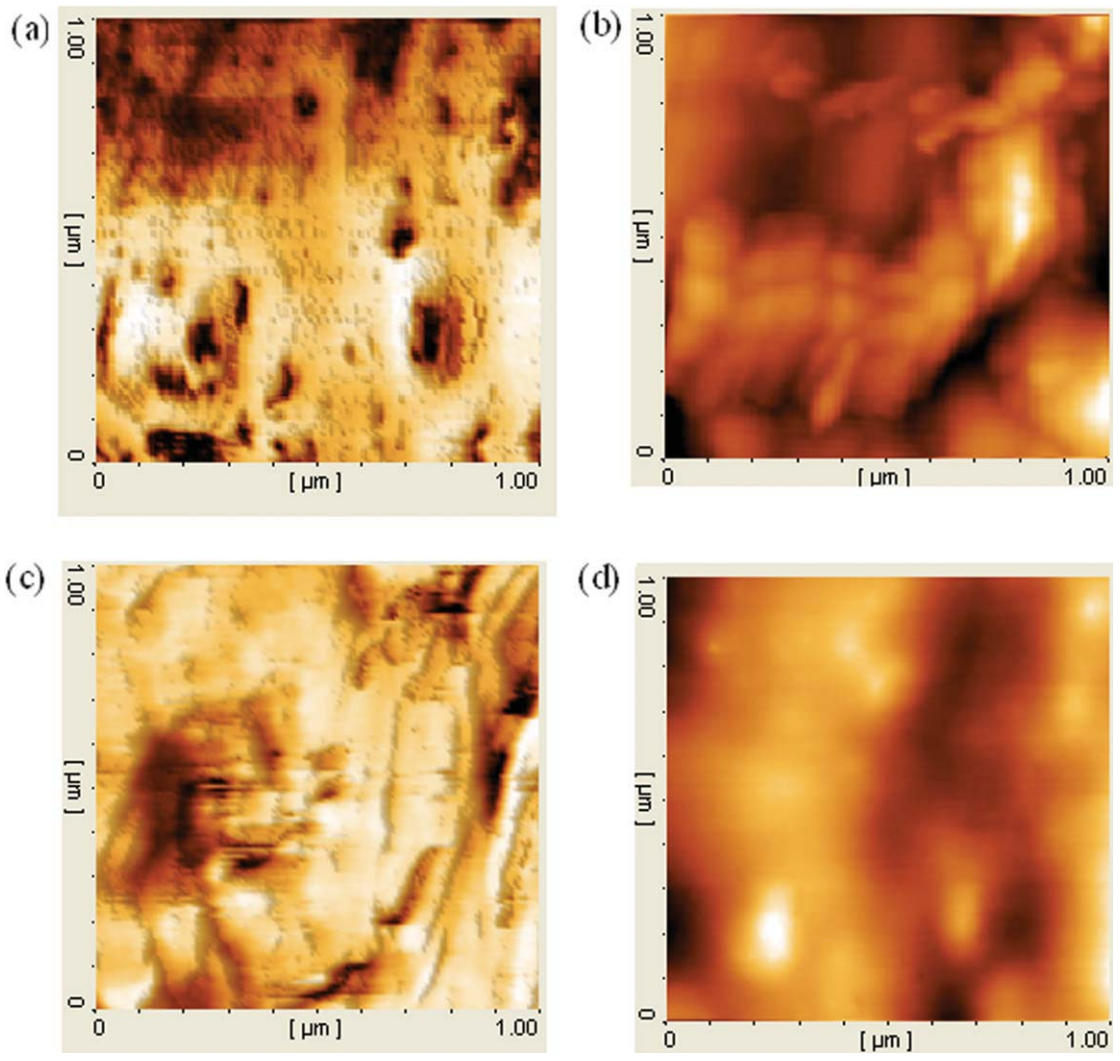

Figure 7 AFM images: (a) phase and (b) topography images of PP4/4/8 and (c) phase and (d) topography images of PP4/2/14 samples. [Color figure can be viewed in the online issue, which is available at wileyonlinelibrary.com.]

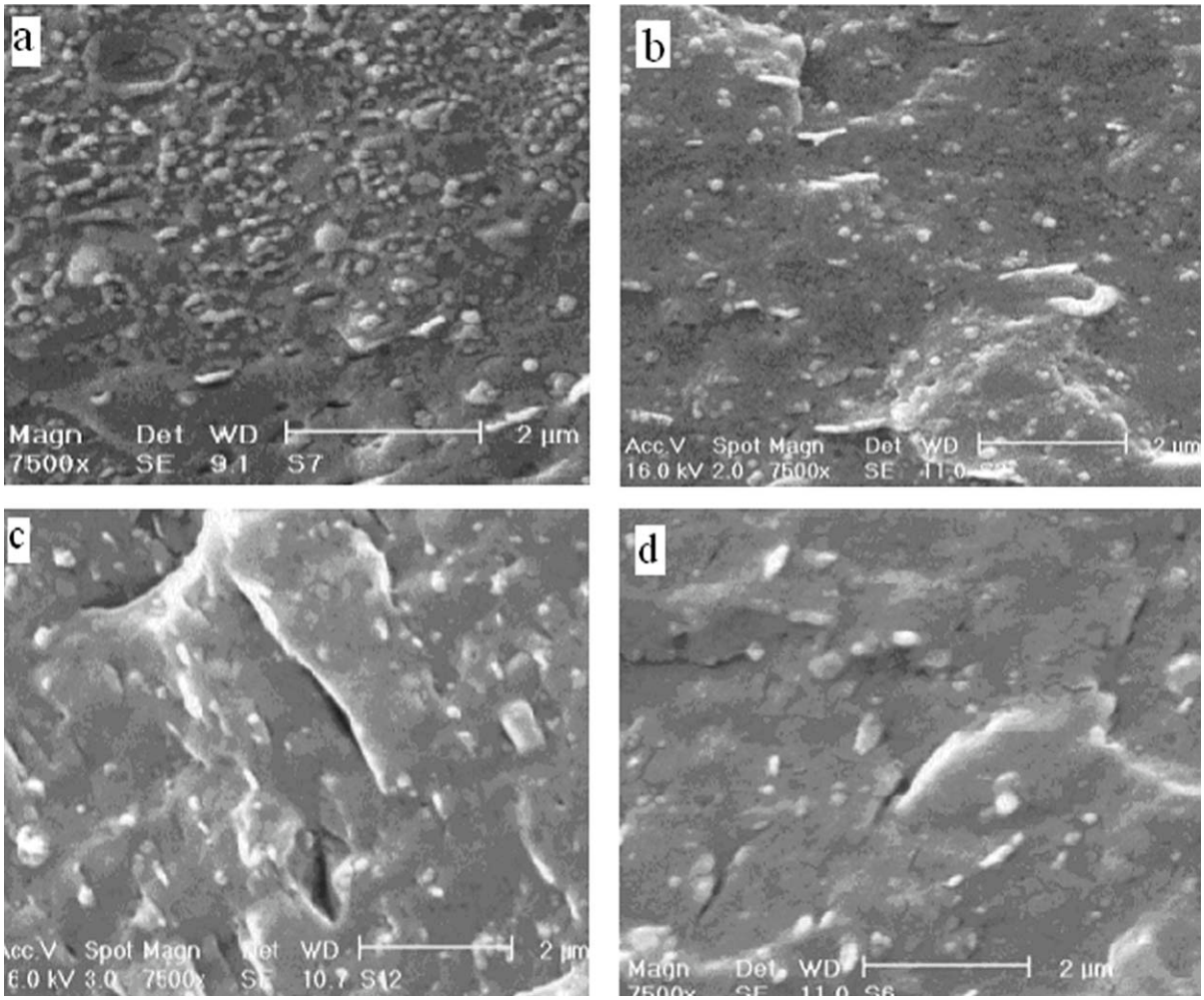

Figure 8 SEM micrographs of (a) PP4/2/14, (b) PP10/2/20, (c) PP10/2/8, and (d) PP10/4/14 samples.

and 2.73 nm, respectively, indicating intercalated structure of nanoclay layers in these samples. Also, the amount of exfoliated layers in nanocomposite is inversely related to the intensity of XRD peak.[32] Mainly, peak intensity in the PP4/4/8 and PP16/4/8 samples decreases, demonstrating a partially exfoliation of nanoclay layers. Therefore, the intercalated/exfoliated morphology for PP4/4/8 and PP16/4/8 samples is observed. XRD patterns of PP4/2/14 and PP4/6/14 samples are also shown in Figure 4(b). For PP4/6/14 sample, an intercalated/exfoliated structure is depicted, but in PP4/2/14 sample, nanoclay layers were completely exfoliated in PP matrix.

To further analyze of the effect of $CaCO_3$ content on the nanoclay structure in ternary nanocomposite, XRD patterns of PP10/6/8 and PP10/6/20 samples are shown in Figure 5(a). The interlayer spacing of nanoclay galleries is 2.54 and 2.63 nm for PP10/6/8 and PP10/6/20 samples, respectively. The peak intensity of PP10/6/20 sample is lower than that of PP10/6/8 sample indicating that more nanoclay layers have been exfoliated in the higher $CaCO_3$ concentration. Also, XRD patterns of PP16/4/8 and PP16/4/20 samples are shown in Figure 5(b). It can be seen that the peak intensity of PP16/4/20 sample is lower than that of PP16/4/8 sample showing the more partially exfoliation of nanoclay layers in high $CaCO_3$ content. Further morphological characterization of prepared samples is presented employing AFM and SEM techniques.

Recently, AFM has received intense attention in the study of nanocomposites morphology because of atomic resolution scale it has.[33–37] However, the studies of lamellar structures should be executed by the high-resolution experimental probes, which can image at the nanometer scale. In AFM images, it is so important to note that any changes in phase images (darker or lighter areas) would not indicate to the variation in the nature of the material because variations in the height of the sample surface can show some darker or lighter area in the phase images.

Figure 6 observes the AFM images of PP4 sample. The phase and topography images of PP4 have a perfect uniform surface confirming the presence of

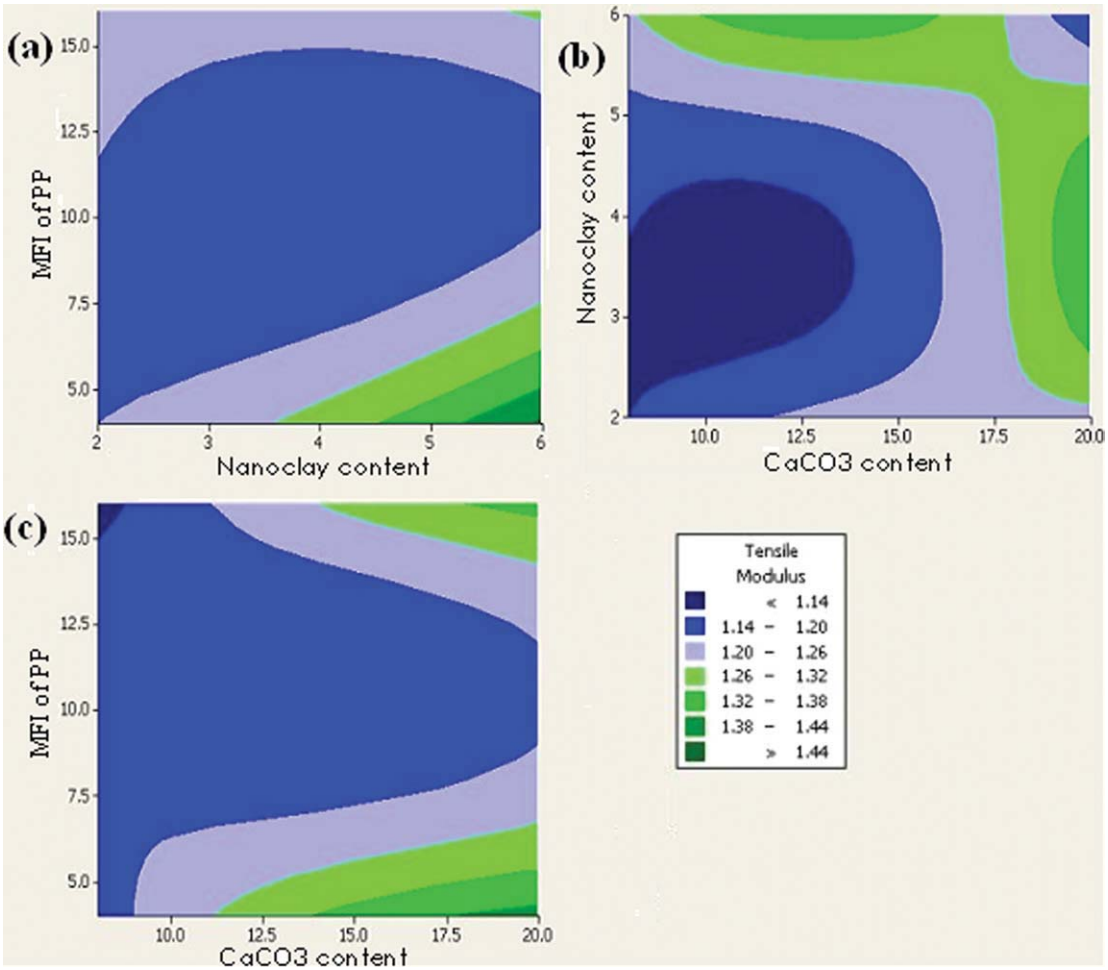

Figure 9 The contour plots of tensile modulus. [Color figure can be viewed in the online issue, which is available at wileyonlinelibrary.com.]

one phase in the sample. Figure 7 illustrates the phase and topography images of PP4/4/8 and PP4/2/14 samples. The darker streaks in the phase image of PP4/4/8 and PP4/2/14 samples show the partially exfoliated nanoclay in PP matrix, whereas the darker spots with higher size can show the dispersed $CaCO_3$ nanoparticles. The thicker darker areas in the phase image of PP4/4/8 can show the clusters of nanoparticles in the PP matrix. It is noting that the rotation of exfoliated nanoclay layers in the PP matrix should be considered. Also, the thicker area may be the intercalated nanoclay in the PP matrix. If the phase image of PP4/2/14 sample is taken into account, the thicker darker area is observed slightly. As mentioned before, XRD patterns indicated no intercalated structure of nanoclay in the PP4/2/14 sample, but mixed intercalated/exfoliated nanoclay was shown in the PP4/4/8 sample.

Further evaluation of morphological properties is performed using SEM micrographs. Figure 8 illustrates SEM micrographs of PP4/2/14, PP10/2/20, PP10/2/8, and PP10/4/14 samples. The homogeneously dispersed nanoparticles (nanoclay and $CaCO_3$) are observed within the PP matrix in the SEM micrographs. The smooth surface of the SEM images shows that any agglomeration of nanoparticles specifically $CaCO_3$ clusters is not found in the samples. The good dispersion of nanoparticles in the polymer matrix is not an easy work because nanoparticles have a tendency to aggregation due to high surface energy. This dispersion indicates to high-quality interface adhesion between PP and nanofillers.

It was discussed before that low MFI of PP induces high shear stress to melt mixture in the extruder leading to well exfoliation of nanoclay with homogeneous dispersion of $CaCO_3$ nanoparticles in PP matrix. The XRD, AFM, and SEM images show the mixed exfoliated/intercalated morphology of nanoclay layers in many samples as well as the dispersion of $CaCO_3$ nanoparticles in the PP matrix.

Response function

By fitting a cubic response surface model as a function of MFI of PP, nanoclay, and $CaCO_3$

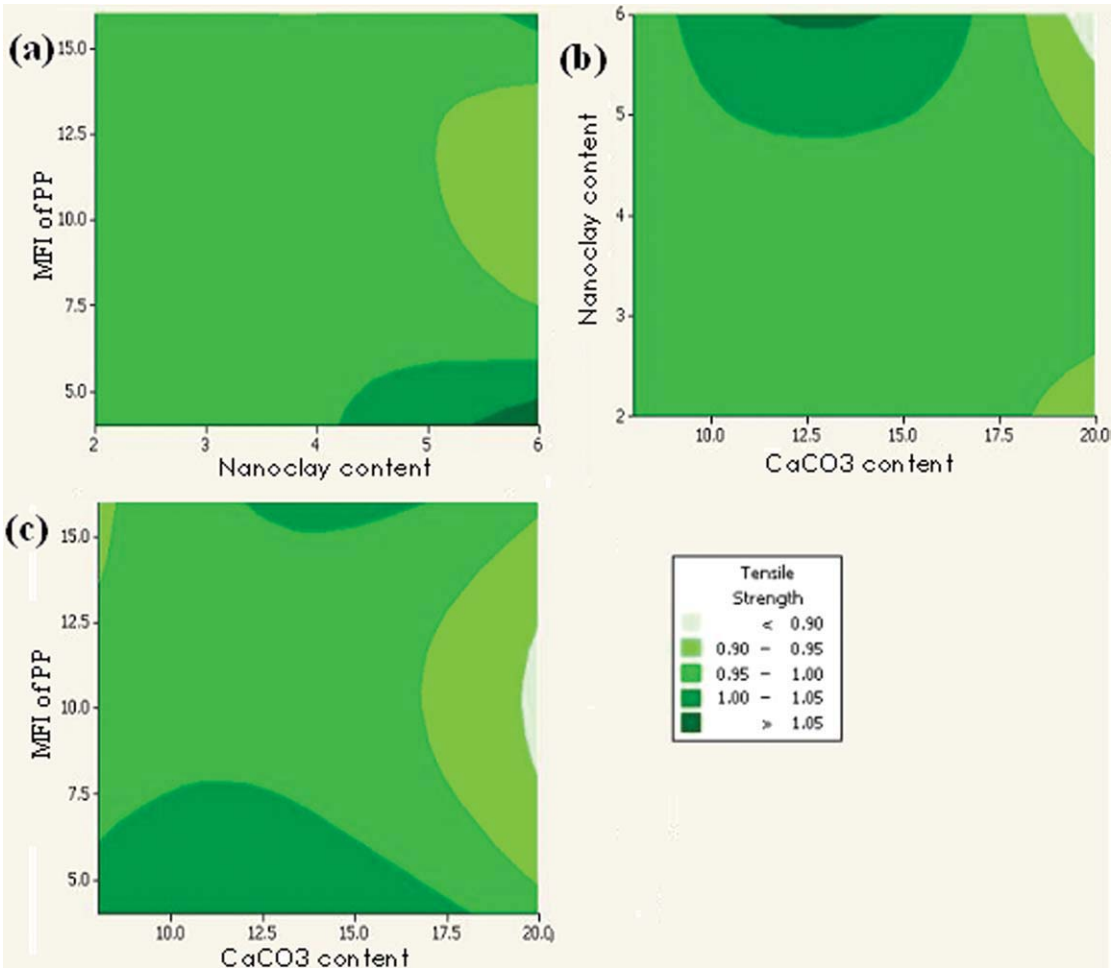

Figure 10 The contour plots of tensile strength. [Color figure can be viewed in the online issue, which is available at wileyonlinelibrary.com.]

concentrations, the response function can be presented as:

$$Y = \beta_0 + \beta_1 x_1 + \beta_2 x_2 + \beta_3 x_3 + \beta_{11} x_1^2 + \beta_{22} x_2^2 + \beta_{33} x_3^2 + \beta_{12} x_1 x_2 + \beta_{13} x_1 x_3 + \beta_{23} x_2 x_3 \quad (2)$$

The values of coefficients for tensile modulus and impact strength are presented in Table IV. The *R*-square value for model of tensile modulus is about 87% showing that the presented model can explain 87% of the variability in the tensile modulus over parameter domain. Also, the *P*-values illustrating the pure quadratic coefficient approximation or a measure of the statistical importance show that $CaCO_3$ content term could has the most significant effect in this model. Moreover, the *P*-value for lack of fit (adequacy of fitted model) is 0.074 suggesting this model adequately fits the tensile modulus results. In addition, the *R*-square value for impact strength function is about 77%. The *P*-value for lack of fit in impact strength model is 0.092 suggesting the high adequacy of fitted model with impact strength data.

Contour plots

The contour plots are useful for creation of desirable response. They show the contribution of two factors simultaneously, and another factor is kept at its average level.

Figure 9(a) shows the contour plot of tensile modulus as a function of MFI of PP and nanoclay content in the $CaCO_3$ content of 14 wt %. It is observed that higher than 38% improvement of the tensile modulus can be obtained using low MFI of PP and nanoclay content of about 6 wt %. Figure 9(b) illustrates that the best results of tensile modulus are achieved in the nanoclay content of 3–4.5 wt % and $CaCO_3$ content of 20 wt % as well as in the highest level of nanoclay content (6 wt %), and $CaCO_3$ content of 10–16 wt %. Figure 9(c) shows that to prepare the PP/nanoclay/$CaCO_3$ ternary nanocomposite with maximum tensile modulus, lower and higher MFI of PP (4 or 16 g/10 min) and $CaCO_3$ content of about 18–20 wt % in the nanoclay content of 4 wt % should be used.

Figure 10 shows the contour plots of tensile strength. As observed in Figure 10(a), the best

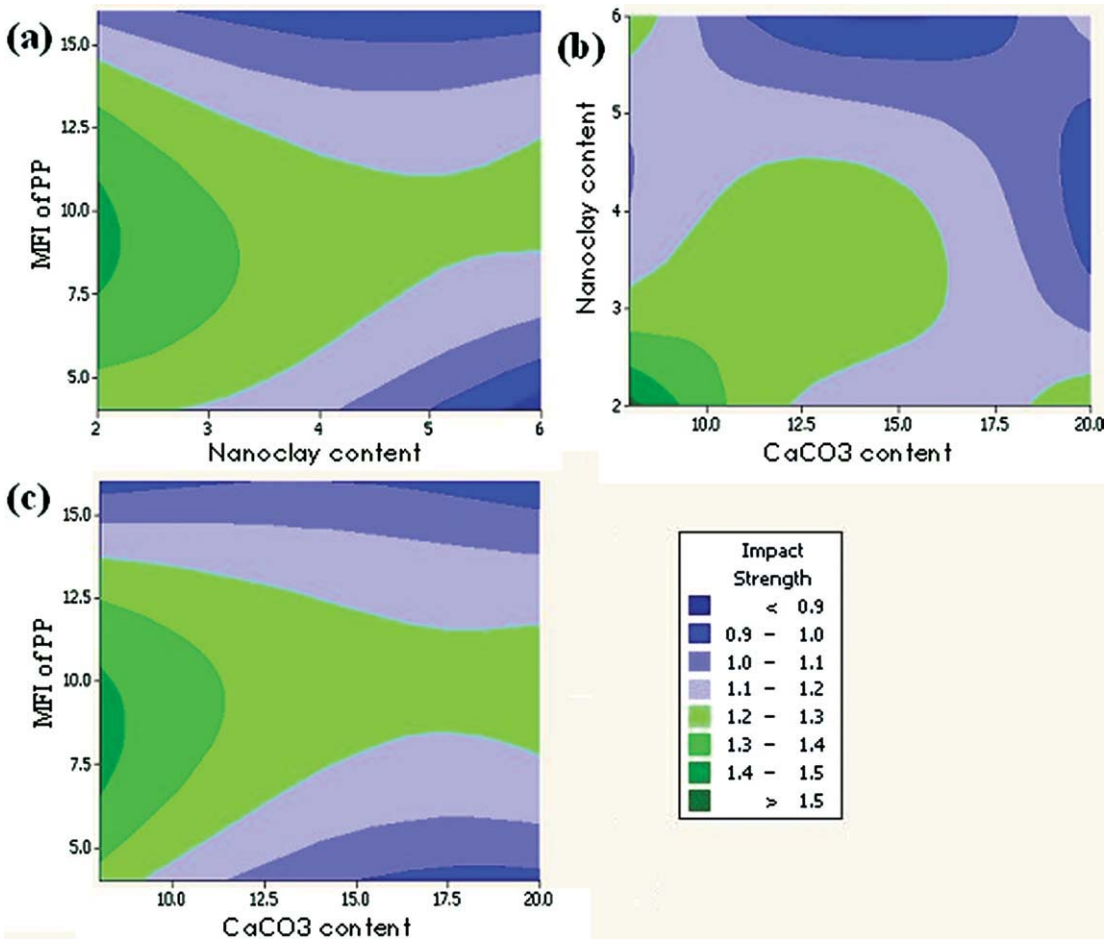

Figure 11 The contour plots of impact strength. [Color figure can be viewed in the online issue, which is available at wileyonlinelibrary.com.]

improvement of tensile strength can be obtained in the lowest and the highest MFI of PP (4 or 16 g/10 min) and nanoclay content of about 6 wt % in the $CaCO_3$ content of 14 wt %. Figure 10(b) indicates that to maximize the tensile strength, higher nanoclay content (6 wt %) and average levels of $CaCO_3$ (12–14 wt %) should be used. Figure 10(c) demonstrates that the worst results of tensile strength are achieved using MFI of PP about 8–12 g/10 min and $CaCO_3$ contents of 20 wt % in the nanoclay content of 4 wt %.

The contour plots of impact strength are presented in Figure 11. Figure 11(a) indicates that to obtain compounds with the best impact results (higher than 40%), PP with MFI of about 8–11 g/10 min and nanoclay content of 2 wt % are required. Figure 11(b) shows the effect of nanofiller contents on the impact strength at medium level of MFI of PP (10 g/10 min). To maximize the improvement of impact strength, the lowest level of nanoclay and $CaCO_3$ contents should be used. Figure 11(c) also indicated that the highest improvement of impact strength is obtained in the $CaCO_3$ content of 8 wt % using MFI of PP, over a range of 7–10 g/10 min.

CONCLUSIONS

Response surface methodology was used to study the effect of three parameters including MFI of PP, nanoclay, and $CaCO_3$ contents on the mechanical properties of PP/nanoclay/$CaCO_3$ nanocomposite. The optimized and the minimum contributions of variables on the tensile modulus and impact strength were determined using contour plots. The results show that the most improvements of tensile modulus and impact strength are obtained in the low and medium levels of MFI, respectively. The addition of nanoclay and $CaCO_3$ has a positive effect on the tensile modulus and low influence on tensile strength but decrease the impact strength. Although the addition of $CaCO_3$ promotes many toughening mechanisms in binary nanocomposites, but in the case of prepared PP/nanoclay/$CaCO_3$ ternary

nanocomposite, the better result of impact strength is observed at low level of $CaCO_3$, because of acting of $CaCO_3$ large clusters as stress concentrators.

The best balanced mechanical properties between 15 designed formulations were obtained using medium level of MFI of PP (10 g/10 min), 2 wt % of nanoclay, and 8 wt % of $CaCO_3$ in which 14% improvement of tensile modulus and 54% enhancement in the impact strength were achieved compared with pure PP10. The XRD, AFM, and SEM images demonstrate the mixed intercalation/exfoliation morphology of nanoclay and the good dispersion of $CaCO_3$ nanoparticles in the prepared ternary nanocomposite.

References

1. Wang, K.; Chen, L.; Wu, J.; Toh, M. L.; Heand, C.; Yee, A. F. Macromolecules 2005, 38, 788.
2. Isik, I.; Yilmazerand, U.; Bayram, G. Polym Compos 2007, 29, 133.
3. Liu, X.; Wu, Q.; Berglund, L. A.; Lindberg, H.; Fanand, J.; Qi, Z. J Appl Polym Sci 2003, 88, 953.
4. Dong, W.; Liu, Y.; Zhang, X.; Gao, J.; Huang, F.; Song, Z.; Tanand, B.; Qiao, J. Macromolecules 2005, 38, 4551.
5. Modesti, M.; Lorenzetti, A.; Bon, D.; Besco, S. Polymer 2005, 46, 10237.
6. Lertwimolnun, W.; Vergnes, B. Polymer 2005, 46, 3462.
7. Weon, J.; Gam, K.; Boo, W.; Sue, H.; Chan, C. J Appl Polym Sci 2006, 99, 3070.
8. Yang, K.; Yang, Q.; Li, G.; Sun, Y.; Feng, D. Mater Lett 2006, 60, 805.
9. Dagani, R. Chem Eng News 1999, 77, 25.
10. Wang, G.; Chen, X. Y.; Huang, R.; Zhang, L. Mater Sci Lett 2002, 21, 985.
11. Levita, G.; Marchetti, A.; Lazzeri, A. Polym Compos 1989, 10, 39.
12. Chen, H.; Wang, M.; Lin, Y.; Chi-Ming, C.; Wu, J. J Appl Polym Sci 2007, 106, 3409.
13. Tang, Y.; Hu, Y.; Zhang, R.; Wang, Z.; Gui, Z.; Chen, Z.; Fan, W. Macromol Mater Eng 2004, 289, 191.
14. Sorrentino, L.; Berardini, F.; Capozzoli, M. R.; Amitrano, S.; Iannace, S. J Appl Polym Sci 2009, 113, 3360.
15. Chen, Y.-D.; Pengand, J.; Lui, W.–B. J Appl Polym Sci 2009, 113, 258.
16. Guand, S.-Y.; Ren, J. Macromol Mater Eng 2005, 290, 1097.
17. Sukigara, S.; Gandhi, M.; Ayutsede, J.; Micklusand, M.; Ko, F. Polymer 2004, 45, 3701.
18. Wang, K. H.; Choi, M. H.; Koo, C. M.; Choi, Y. S.; Chung, I. J. Polymer 2001, 42, 9819.
19. Montgomery, D. C. Design and Analysis of Experiments, 6th ed.; Wiley: New York, 2005; p 405.
20. Box, G. E. P.; Draper, N. R. Empirical Model-Building and Response Surfaces; Wiley: New York, 1987; p 477.
21. Kim, K. N.; Kimm, H.; Lee, J. W. Polym Eng Sci 1963 2001, 41.
22. Bousmina, M. Macromolecules 2006, 39, 4259.
23. Ray, S. S.; Okamoto, M. Prog Polym Sci 2003, 28, 1539.
24. Dasari, A.; Yu, Z.-Z.; Yang, M.; Zhang, Q. -X.; Xieand, X. -L.; Mai, Y. -W. Compos Sci Technol 2006, 66, 3097.
25. Zhou, H.; Rong, M.; Zhang, M.; Ruan, W. H.; Friedrich, K. Polym Eng Sci 2007, 47, 499.
26. Svoboda, P.; Zeng, C.; Wang, H.; Lee, L. J.; Tomasko, D. L. J Appl Polym Sci 2002, 85, 1562.
27. Zhu, J.; Wilkie, C. A. Polym Int 2000, 49, 1158.
28. Wang, Y.; Chen, F. B.; Wu, K. C. J Appl Polym Sci 2004, 93, 100.
29. Peltola, P.; Lipakka, E.; Vuorinen, J.; Syrja, S.; Hanhi, K. Polym Eng Sci 2006, 46, 995.
30. Fornes, T. D.; Yoon, P. J.; Keskkula, H.; Paul, D. R. Polymer 2001, 42, 9929.
31. Chen, J.; Wang, G.; Zeng, X.; Zhao, H.; Cao, D.; Yun, J.; Tan, C. K. J Appl Polym Sci 2004, 94, 796.
32. Alexandre, M.; Dubois, P. Mater Sci Eng 2000, 28, 1.
33. Ballinas-Casarrubias, L.; Terrazas-Bandala, L. P.; Ibarra-Gomez, R.; Mendoza-Duarte, M. E.; Manjarrez-Nevarez, L.; Gonzalez-Sanchez, G. Polym Adv Technol 2006, 17, 991.
34. Maiti, M.; Bhowmick, A. K. Polymer 2006, 47, 6156.
35. Ma, D.; Akpalu, Y. A.; Li, Y.; Siegel, W.; Schadler L. J Polym Sci B: Polym Phys 2005, 43, 488.
36. Chan, C. M.; Wu, J. S.; Li, J. X.; Cheung, Y. K. Polymer 2002, 43, 2981.
37. Raghavan, D.; Gu X.; Nguyen, T.; VanLandingham M.; Karim A. Macromolecules 2000, 33, 2573.